

# Optimized Signaling Method for High-Speed Transmission Channels with Higher Order Transfer Function

Břetislav Ševčík<sup>1</sup>, Lubomír Brancík<sup>2</sup>, Michal Kubíček<sup>3</sup>

<sup>1</sup>Technology Centre, ABB s. r. o., Videnska 117, 619 00, Brno, Czech Republic, [bretislav.sevcik@cz.abb.com](mailto:bretislav.sevcik@cz.abb.com)

<sup>2</sup>Department of Radio Electronic, Faculty of Electrical Engineering and Communication, Brno University of Technology, Technická 12, 616 00, Brno, Czech Republic, [brancik@feec.vutbr.cz](mailto:brancik@feec.vutbr.cz)

<sup>3</sup>Department of Radio Electronic, Faculty of Electrical Engineering and Communication, Brno University of Technology, Technická 12, 616 00, Brno, Czech Republic, [kubicek@feec.vutbr.cz](mailto:kubicek@feec.vutbr.cz)

In this paper, the selected results from testing of optimized CMOS friendly signaling method for high-speed communications over cables and printed circuit boards (PCBs) are presented and discussed. The proposed signaling scheme uses modified concept of pulse width modulated (PWM) signal which enables to better equalize significant channel losses during data high-speed transmission. Thus, the very effective signaling method to overcome losses in transmission channels with higher order transfer function, typical for long cables and multilayer PCBs, is clearly analyzed in the time and frequency domain. Experimental results of the measurements include the performance comparison of conventional PWM scheme and clearly show the great potential of the modified signaling method for use in low power CMOS friendly equalization circuits, commonly considered in modern communication standards as PCI-Express, SATA or in Multi-gigabit SerDes interconnects.

Keywords: High-speed signaling, equalization, pulse-width modulation, signal integrity, channel loss, multi-gigabit.

## 1. INTRODUCTION

Multi-GB/s signaling is a part of each present day communication standard. For the next generation of signaling standards, developed by OIF and IEEE, the usage of PAM4 signaling at data rates over 50 Gbps is seriously considered [1]. The main idea is to maintain a hardware structure of the current transmission channels and increase the data rate. Thus, the significant cost advantages can be reached. There are a few papers which seriously discuss the possibility to achieve higher data rates using multi-level signaling methods over the backplanes and copper cables [2]-[5].

Due to the frequency-dependent channel impairment variation a proper signaling over lossy transmission channels cannot exist without multi-Gb/s transceivers including equalization circuits. This is still an area of ongoing research for transmission channels such as backplane traces or coaxial cables. As data rate goes beyond 40 Gbps, multilevel signaling techniques as PAM4 signaling is gaining attraction, especially for backplane applications. In frequency domain, the PAM4 signaling requires half the bandwidth than a conventional non-return-to-zero (NRZ) signaling. For total signal swing which is kept constant, the level spacing for PAM4 is 1/3 of NRZ. Thus, the signal-to-noise (SNR) loss calculation can be defined as

$$SNR = 20 \cdot \log\left(\frac{1}{3}\right) = -9.54 \text{ dB} \quad (1)$$

In this case the signal degradation due to the channel losses can cause a complete closing of the eye diagram earlier than in the case of NRZ signaling. Especially, high frequency content which is significantly greater in PAM4 due to the higher number of signal transitions should be a problem. For example, if we want to achieve transmission rate 30 Gbps, the Nyquist frequency for NRZ is 15 GHz, while for PAM4 is 7.5 GHz. There are a few potential problems which should be taken into account. In the first case conventional equalization methods based on amplitude emphasis/de-emphasis may not be sufficient for such channel loss compensation in modern CMOS low power circuits where voltage amplitude swing is reduced. The second case shows potential problems if the alternative PWM equalization techniques are used. The PWM signaling scheme has higher frequency content than conventional signal with amplitude emphasis. Thus, the requirements of lower Nyquist frequency for PAM4 signaling paradoxically can cause that low pass effect of transmission channel is weaker than in the case of NRZ signaling and additional frequency content at the output of transmission channel cause significant eye opening reduction. The final results and performance of both equalization techniques are also

strongly dependent on the transfer function of transmission channel. In this paper an alternative signaling scheme is presented and compared with conventional equalization methods to judge the possible better equalization of higher order transmission channels.

## 2. TRANSMISSION CHANNEL PROPERTIES

During the analysis of signaling scheme performance two types of transmission channels were used. Two analyzed transmission channels are shown in Fig.1. In the first case, the transmission channel optimized for units of gigabits transfer rates (channel A) is used. The second case shows channel with better spectral purity at higher frequencies suitable for transfer rates of tens of gigabits (channel B). The main idea is to show comprehensively better properties of analyzed signaling scheme in situations where significant eye open reduction can occur.

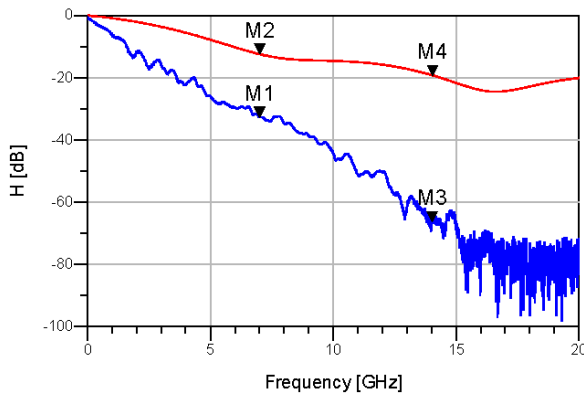


Fig.1. Two analyzed transmission channels: blue line (channel A, marked by M1) – measured backplane channel of Texas Instruments development board with higher losses at higher frequencies, red line (channel B, marked by M2) – channel better optimized for multi-GB/s signaling.

To demonstrate the loss effects of both transmission channels, several types of signal transmission have been carried out. In the first case, the PAM4 signaling was arranged. As can be seen from Fig.1., the Nyquist frequency (7 GHz) for 28 Gbps transfer rate is marked as M1 for channel A and M2 for channel B. The marker M1 shows signal attenuation -32.73 dB and the marker M2 shows signal attenuation -12.44 dB. Both output eye diagrams are shown in Fig.2. It is obvious that output eye diagram for channel A is almost closed. Note that the receiver has enabled DFE (decision feedback equalizer) equalization like during PCI Express signaling. Thus, the channel losses over 30 dB cannot be successfully equalized without additional signal rearrangement at the transceiver side. Usually, transceiver pre-emphasis circuits based on the FIR filtering are used [6]-[8]. However, the requirement of modern CMOS signaling standards shows the tendency to reduce signal amplitude swing. There are a few new approaches based on the PWM signaling scheme which show better signal adaptation to the lossy channel [9]-[11]. Especially in the paper [10] there are also thoughts about multi-level

variants of PWM equalization techniques. However, our target is to achieve better high-order channel loss compensation by adaptation of conventional PWM scheme to the second order variant. In the papers [12]-[14] the effect of additional signal shaping on the performance of PWM signaling scheme is clearly demonstrated. However, the performance can be increased by modification of conventional PWM scheme to the second order signaling PWM scheme for better adaptation to the transmission channels with higher-order transfer functions, typically long coaxial cables, PCB backplanes with signal discontinuities due to the necessity to use vias in design, etc. More details in section 3.

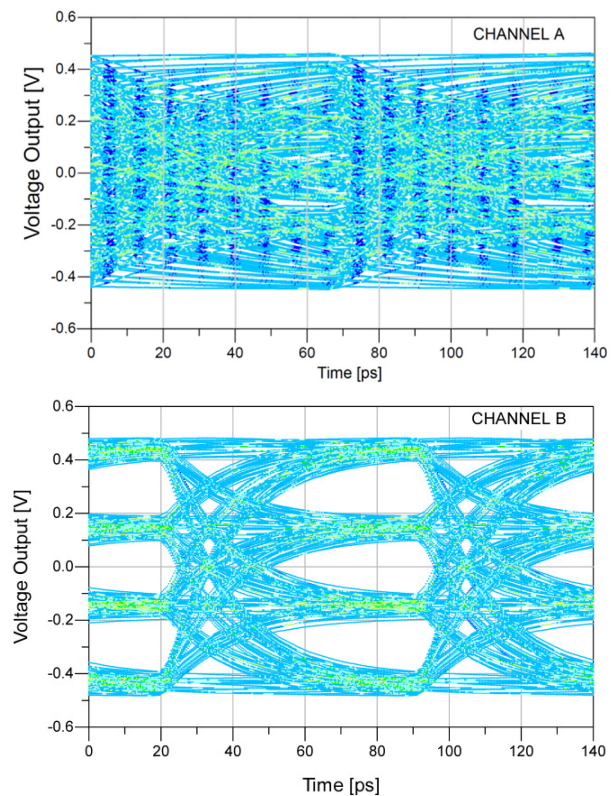


Fig.2. Output eye diagrams, PAM4 signaling, DFE receiver equalization enabled, 28 Gbps.

In the second case the effect of channel losses during the NRZ signaling is demonstrated. The Nyquist frequency is hereby shifted to 14 GHz. This situation is also listed in Fig.1. The marker M3, which represents the losses of channel A, shows signal attenuation -66.3 dB. That is more than double compared to the previous case. On the other hand, channel B shows signal attenuation only -19.3 dB, see marker M4 in Fig.1. Also note that channel A shows at Nyquist frequency 14 GHz significant increase of noise content and probably there is also own channel limit for data signaling. All output eye diagrams are listed in Fig.3. The output eye diagram for channel B shows still good performance also for NRZ signaling. Channel A without DFE equalization at the receiver's side has a completely closed eye diagram. After activation of DFE equalizer a significant improvement in the eye opening is visible.

However, there are present strong jitter and additional signal discontinuities caused by significant noise content increase which degrade the resulting eye opening.

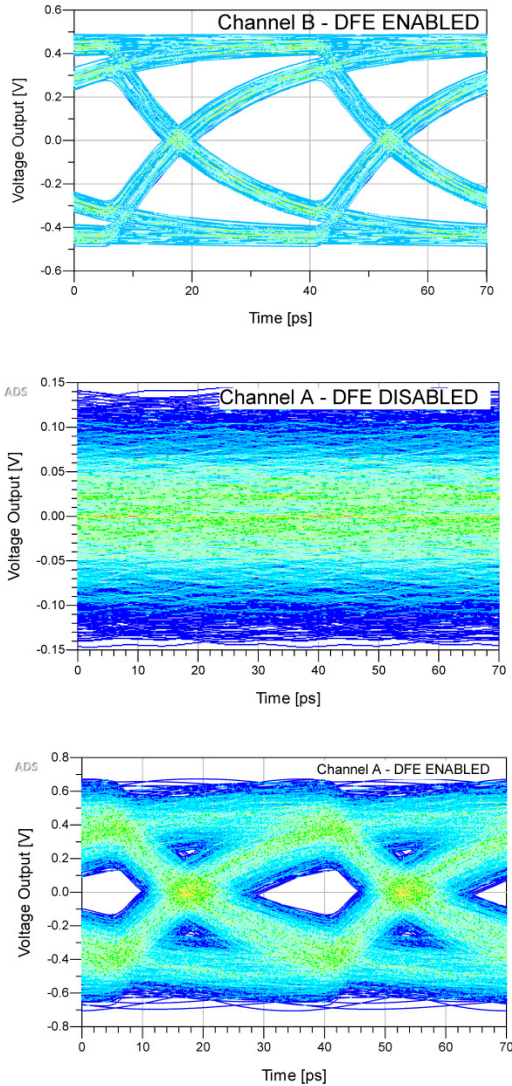


Fig.3. Output eye diagrams, NRZ signaling, 28 Gbps.

### 3. SIGNALING SCHEME

In this section a second order modification of conventional PWM scheme is presented. The coefficients for time domain simulation are defined as  $dc_1 \in \{0 \dots 0.5\}$  and  $dc_2 \in \{0.5 \dots 1\}$ . In this case it is not possible to use one coefficient as in a conventional PWM scheme because optimal results of signal shaping require different coefficient setting. Optimal coefficient setting for the second order pulse-width modulated scheme (PWM-2) is strictly dependent on overall channel impulse response. Due to more variability in PWM-2 pulse shaping, better adaptation to different types of transmission channels may be achieved. As can be seen in Fig.4. and Fig.5. the optimal setting of both duty cycle coefficients can result in significant intersymbol interference reduction. This effect can be achieved for transmission channels with higher losses in relation to the considered transmission rate, see example of transmission channel

with significant reduced bandwidth parameter on  $BW_{3dB} = 250$  MHz, where the optimal duty cycle coefficients are  $dc_1 = 29\%$  and  $dc_2 = 79\%$ . Significant jitter reduction for PWM-2 signaling is obvious; compare all eye diagrams in Fig.4. However, the significant amplitude reduction in the case of PWM-2 is evident. It can be a problem if the noise margin is higher than the residual signal amplitude. Function  $p_{pwm-2}(t)$  in the time domain can be simply formulated as

$$p_{pwm-2}(t) = \begin{cases} 0 & t < 0 \\ 1 & 0 \leq t < dc_1 \cdot T_b \\ -1 & dc_1 \cdot T_b < t \leq \frac{1}{2} \cdot T_b \\ -1 & \frac{1}{2} \cdot T_b < t \leq dc_2 \cdot T_b \\ 1 & dc_2 \cdot T_b < t \leq T_b \\ 0 & t > T_b \end{cases}, \quad (2)$$

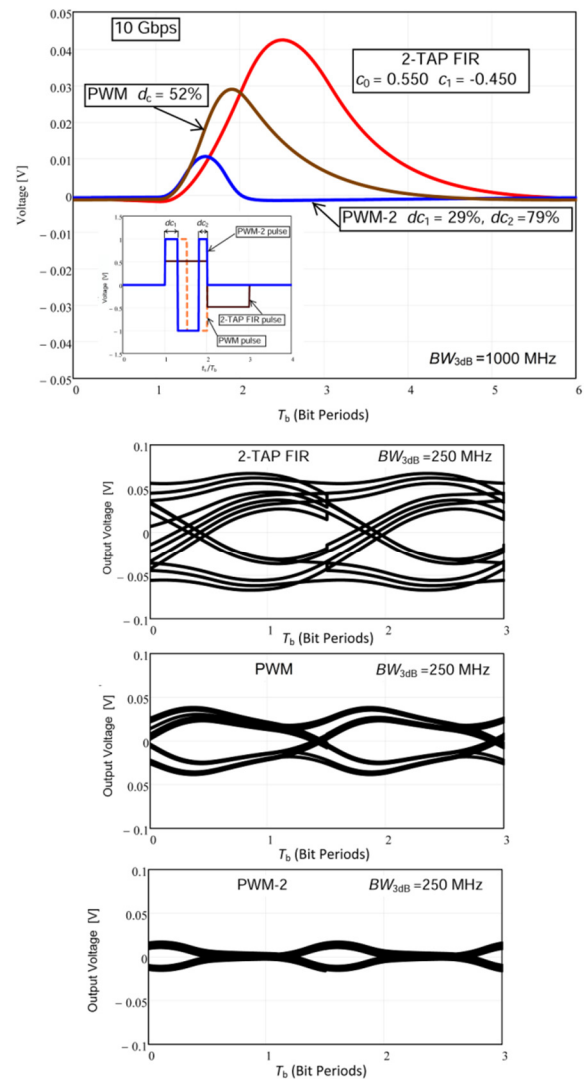


Fig.4. Time-domain analysis: a) impulse responses for FIR, PWM and PWM-2 pulse shaping, b) eye diagrams to evaluate signaling performance after passing through the channel with significant bandwidth restriction.

Fig.5. illustrates both PWM and PWM-2 pulse configuration. It is obvious that output 8 Gbps data stream which passes through the channel with bandwidth restriction parameter  $BW_{3dB} = 1000$  MHz has pulse shaping similar to raised cosine PWM shaping for PWM-2 signal at the channel input; compare pulse shaping in [14] with output data stream in Fig.5. The original idea of using raised cosine shaping for time-domain pre-emphasis techniques was for the first time published in research papers [14], [15].

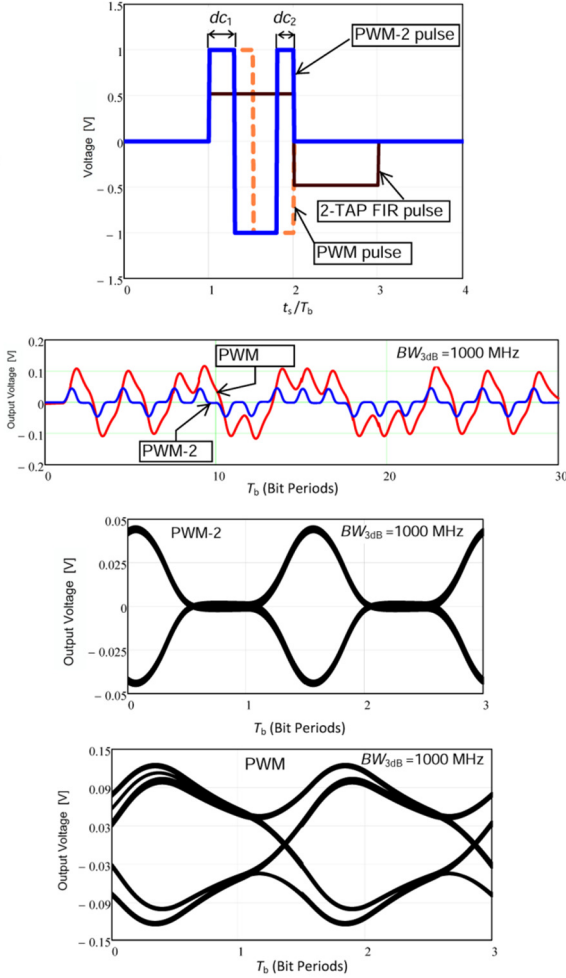


Fig.5. Time-domain analysis: PWM-2 pulse shaping with channel output bit stream demonstration and the relevant eye diagrams for both PWM and PWM-2 signaling techniques.

#### 4. FREQUENCY DOMAIN PERFORMANCE

For meaningful comparisons of previously presented signaling techniques with newly proposed signaling method the power spectral density (PSD) is calculated. The voltage scheme is normalized again to  $\pm 1$  V. The spectrum  $P_{pwm-2}(\omega)$  of the PWM-2 pulse is calculated through Fourier transform of  $p_{pwm-2}(t)$  as

$$P_{pwm-2}(\omega) = \int_{-\infty}^{\infty} p_{pwm-2}(t) \cdot e^{-j\omega t} dt = \int_{-\frac{T_b}{2}}^{-dc_1 T_b} e^{-j\omega t} dt - \int_{-dc_1 T_b}^{(dc_2-0.5)T_b} e^{-j\omega t} dt + \int_{(dc_2-0.5)T_b}^{\frac{T_b}{2}} e^{-j\omega t} dt \quad (3)$$

After simplification:

$$P_{pwm-2}(\omega) = \frac{2 \cdot e^{-j\omega(dc_2-0.5)T_b} + e^{j\omega T_b} - 2 \cdot e^{j\omega dc_1 T_b} - e^{-j\omega 0.5 T_b}}{j\omega} \quad (4)$$

Now we can calculate the power spectral density  $PSD_{pwm}$  for the PWM-2 filter:

$$PSD(\omega) = \frac{|P(\omega)|^2}{T_b} \sum_{k=-\infty}^{k=\infty} R(k) \cdot e^{j\omega k T_b} \quad (5)$$

$$PSD(\omega) = \frac{|-2j \cdot e^{-j\omega(dc_2-0.5)T_b} - j \cdot e^{j\omega T_b} + 2j \cdot e^{j\omega dc_1 T_b} + j \cdot e^{-j\omega 0.5 T_b}|^2}{\omega^2 \cdot T_b} =$$

$$= \frac{|-2 \cdot e^{-j\omega(dc_2-0.5)T_b} - e^{j\omega T_b} + 2 \cdot e^{j\omega dc_1 T_b} + e^{-j\omega 0.5 T_b}|^2}{\omega^2 \cdot T_b} =$$

$$= \frac{1}{\omega^2 T_b} \left\{ \left[ 2 \cos \omega dc_1 T_b - 2 \cos(\omega(dc_2 - 0.5)T_b) + \cos \omega 0.5 T_b - \cos \omega T_b \right]^2 + \right.$$

$$\left. + \left[ 2 \sin \omega dc_1 T_b + 2 \sin(\omega(dc_2 - 0.5)T_b) - \sin \omega 0.5 T_b - \sin \omega T_b \right]^2 \right\} \quad (6)$$

where  $P(\omega)$  is the Fourier transform of  $p(t)$  (in this case it is  $p_{pwm-2}(t)$ ) and  $R(k)$  is the autocorrelation function for a polar NRZ signaling ( $R(k)$  is the same for PWM as for polar NRZ) and is completely calculated in [16].

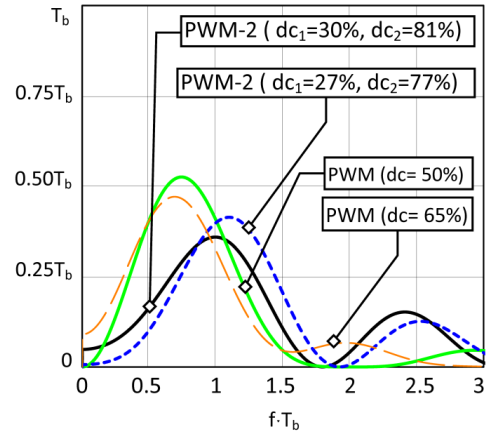


Fig.6. PSD calculation for PWM-2 pulse.

If (6) is taken into account for calculation of  $PSD_{pwm-2}$ , following graphical outputs, as shown in Fig.6., are obtained. Note that the normalization for bit periods on x-axis and y-axis is for better understanding of the performance of the new proposed pulse. The  $dc$  coefficients are set for equalization of transmission channel with higher losses. The spectrum of PWM-2 pulse is even more boosted at higher frequencies than conventional PWM pulse above Nyquist frequency (0.5 on the x axis). It can be an important factor for higher performance to compensate more lossy channels. The main disadvantage of the PWM method proposed in [16] is that the output pre-distorted signal has many harmonic high frequency components. In the case of PWM-2 pulse also significant high frequency content can be expected but due to the ability of higher loss compensation

the final signal level where equalization will be done is lower than for the conventional PWM filter. Thus, a stronger low pass effect of the transmission channel will be expected. Finally, this effect may contribute to the higher loss compensation of PWM-2 filter with possibility of sustainable eye opening.

The transfer function for new presented PWM-2 filter can be calculated similarly as in the case of PWM filter [16]. For relevant comparison of both types of filters the spectrum of normal polar NRZ pulse of width  $T_b$  and height 1 is used for normalization of both functions and the final expression is defined as (7) below.

$$H_{PWM-2}(\omega) = \frac{P_{pwm-2}(\omega)}{P_{NRZ}(\omega)} \quad (7)$$

The equation for transfer function can be rewritten as:

$$H_{PWM-2}(j\omega) = \frac{P_{pwm-2}(j\omega)}{P_{NRZ}(j\omega)} = \frac{2 \cdot e^{-j\omega(dc_2-0.5)T_b} + e^{j\omega T_b} - 2 \cdot e^{j\omega dc_1 T_b} - e^{-j\omega 0.5 T_b}}{e^{j\omega 0.5 T_b} - e^{-j\omega 0.5 T_b}} \quad (8)$$

Taking the modulus yields:

$$|H_{PWM-2}(\omega)| = \frac{\sqrt{[2 \cos \omega(dc_2-0.5)T_b + \cos \omega T_b - 2 \cos \omega dc_1 T_b - \cos \omega 0.5 T_b]^2 + [-2 \sin \omega(dc_2-0.5)T_b + \sin \omega T_b - 2 \sin \omega dc_1 T_b + \sin \omega 0.5 T_b]^2}}{2 \cdot |\sin \omega 0.5 T_b|} \quad (9)$$

This function is illustrated in Fig.7. for several values of  $dc_1$ . The second coefficient  $dc_2$  is set to the value which corresponds with the necessity of higher intersymbol interference compensation. A precondition therefore is that the pulse response of the channel is formed by long tail which does affect more bit periods. One of the evaluated parameters is low-frequency compensation; compare Table 1. and Table 2. It is obvious that PWM-2 filter achieves worse performance during compensation of less lossy channels. On the other hand the ability to achieve better loss compensation results for more channels with significant bandwidth restriction is better almost by 26 %.

Finally, the equalized channel transfer function can be calculated for FIR filters and both PWM and PWM-2 filters. As it is analyzed in section 3, a theoretical first-order channel with significant bandwidth restriction is sufficiently equalized by using all three equalization techniques. However, a real cable or PCB trace, especially with additional signal discontinuities, does not have a first order transfer function. From the analysis depicted below it is obvious that the higher order transfer functions, typical for multilayer boards where vias occur, can still be equalized with PWM and PWM-RC pre-emphasis with better results than by using conventional 2-Tap FIR filter. The equalized transfer function is calculated by taking into account the measured results presented in section 2, concretely channel A response which exhibits more losses on the considered Nyquist frequency for 10 Gbps transmission rate  $f_N = 5$  GHz. In this case the channel losses exceed 30 dB. This is the limitation of a conventional PWM scheme where a maximum loss compensation about 30 dB was achieved

[16]. Now flatness in the frequency interval  $[0, f_N]$  can be clearly determined. The channel response for FIR filter is only flat to within 12 dB. It is obvious that FIR filter is not reliable to equalize such high losses. The channel response for PWM filter shows the flatness only 7 dB. In the case of the new proposed signaling scheme PWM-2, flatness is achieved with less than 3 dB difference between low frequency signal level and high frequency signal level. It can be clearly seen from Fig.8. that the PWM-2 filter is able to “almost eliminate” or in other words equalize higher channel losses. Thus, the bandwidth where the signal reduction is 3 dB is extended over the all analyzed range of filtration from 0 to  $f_N$ . Note that better equalization is achieved on the lower signal level. Thus, the decisive factor for effective using of the PWM-2 equalization lies also in the current receiver sensitivity and in the current noise content which occurs during the equalization.

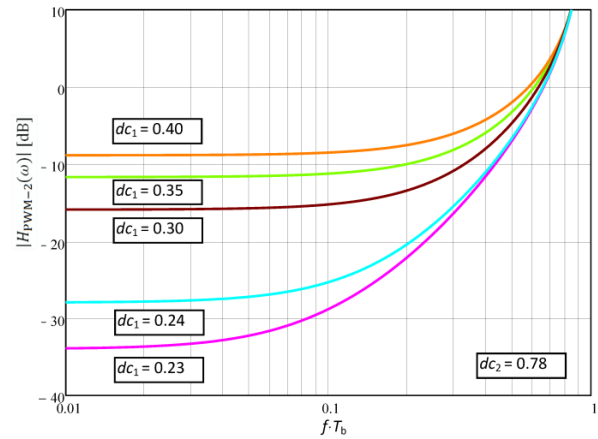


Fig.7. Calculated magnitude of PWM-2 filter transfer. Note that  $f_N$  is at 0.5 on the x-axis.

Table 1. PWM filter loss compensation.

Channel $BW_{3dB}$ [MHz]	$dc$ [%]	LF compensation [dB]
2000	61	13
1000	57	17
500	54	22
250	52	27
The maximum theoretical compensation is 36 dB, $dc = 50\%$		

Table 2. PWM-2 filter loss compensation.

Channel $BW_{3dB}$ [MHz]	$dc_1$ [%]	$dc_2$ [%]	LF compensation [dB]
2000	36	83	9
1000	29	79	16
500	23	79	28
250	23	78	34
The maximum theoretical compensation is 54 dB, $dc_1 = 22\%$ , $dc_2 = 78\%$			

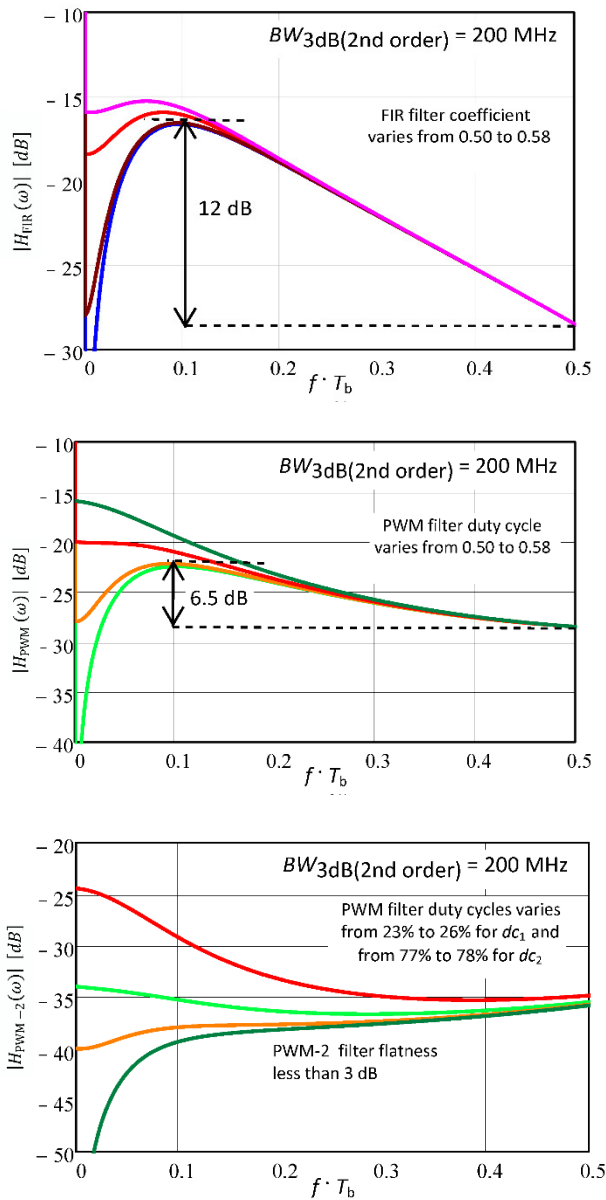


Fig.8. Equalized transfer function, second order channel used: FIR filter, PWM filter and PWM-2 filter. Note that  $f_N$  is at 0.5 on the x-axis.

5. EXPERIMENTAL IMPLEMENTATIONS

For the demonstration of higher order transmission channel loss compensation two types of transmission channels are analyzed. In the first case test channel 1 is represented by 150 m long coaxial cable RGC54. The second case test channel 2 is represented by 100 m long low cost coaxial cable RG174/U. As can be seen from the measured channel attenuation characteristic in Fig.9., the channel losses are significant since of MHz frequencies. Thus, the ratio between the maximum transfer rate and channel losses at 3 dB signal level is similar as in the case of simulation with higher transfer rates. For example, if we take into account the Nyquist frequency for achievable transfer rates, Nyquist frequency 225 MHz for applied transfer rate 450 Mbps can be deduced.

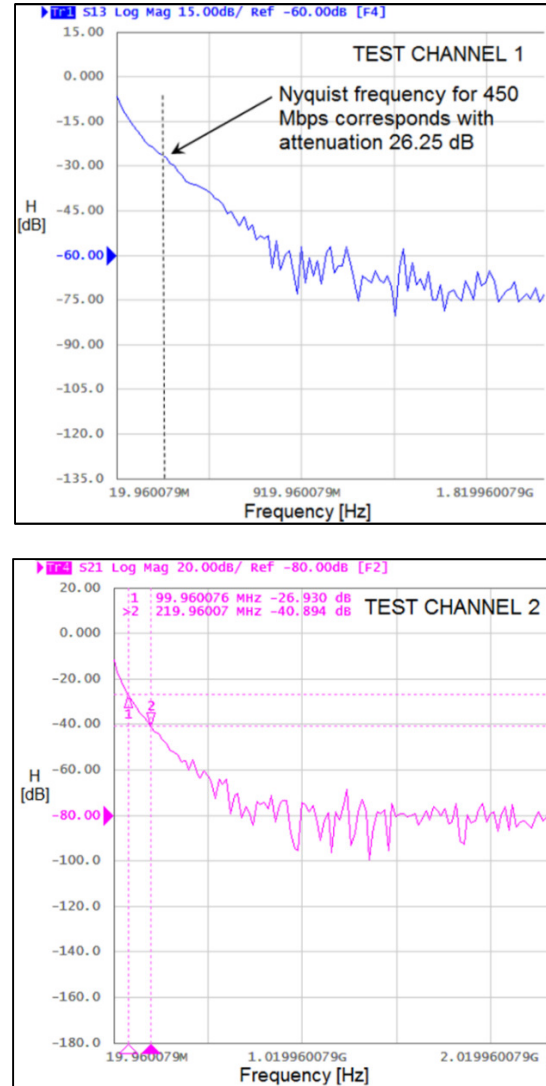


Fig.9. Channel attenuation of analyzed low cost coaxial cables.

In MathCAD simulation the transfer rates from 6 Gbps to 10 Gbps are mainly used for channel losses. It corresponds with Nyquist frequencies from 3 GHz to 5 GHz.  $BW_{3dB}$  coefficients are set to values from 150 MHz to 500 Hz. Thus, the ratio for 4 GHz Nyquist frequency and  $BW_{3dB} = 250$  Hz is 1:16. For Nyquist frequencies deducted from practically implemented transfer rates and  $BW_{3dB} = 12$  MHz the ratio varies from 1:8 to 1:19. Moreover, as was pointed out in previous analyses the main destructive effect on signal shaping has conductive losses as a dominant factor of overall channel losses. Thus, the realized measurements have high predictive value for overall performance evaluation of compared equalization techniques.

The FPGA implementation was used for general realization of signaling PWM techniques. In Fig.10. the principle of FPGA implementations is illustrated. Development board with XUPV5 circuit Virtex-5 (XC5VLX110T) was configured. The digital clock manager (DCM) represents an electronic component available on FPGAs (notably produced by Xilinx producer), mainly used

for manipulating with clock signals inside the FPGA and to avoid clock skew errors in the circuit. Main functions of DCM are multiplying or dividing an incoming clock from external source to the FPGA, for example from Digital Frequency Synthesizer. Thus, SMA\_CLK\_0 clock is adjusted in two steps to generate SMA\_CLK\_1 clock and SMA\_CLK\_2 clock. For the first order PWM signaling only SMA\_CLK\_1 clock is needed. For the second order PWM-2 signaling an additional SMA\_CLK\_2 clock is added. Finally, input data stream DATA\_IN is merged through XOR with both PWM clocks.

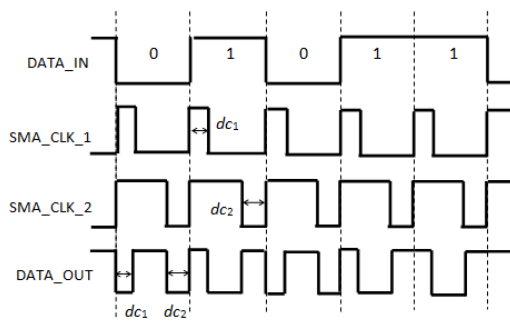
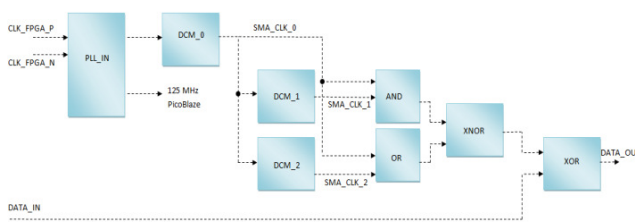


Fig.10. Principle of PWM-2 equalization technique: signaling circuit concept for FPGA implementations and signal diagram.

In the first case, the performance of both PWM and PWM-2 equalization methods for a lower transmission rate of 200 Mbps are compared, see Fig.11. and Fig.12. The test channel 2 shows attenuation about 27 dB at Nyquist frequency. The dc coefficient of conventional PWM pulse is set to almost maximum. However, the loss compensation is still sufficient. After comparing both eye diagrams for PWM and PWM-2 data streams it can be found that due to a better possibility to set appropriate pulse shaping in PWM-2 configuration the higher eye opening is achieved. Note that the jitter and noise parameters are worst for PWM-2 signaling.

In the second case, the transmission rate was increased by more than 50 % and both PWM methods were compared on test channel 1. It is necessary to keep in mind that transmission channel completely closes eye diagram for conventional NRZ signaling. It is obvious that Nyquist frequency for higher transmission rates is situated in an area where channel losses reach almost 30 dB like in the previous case. A comparison of the performance of both signaling techniques shows better results for PWM-2 pulse.

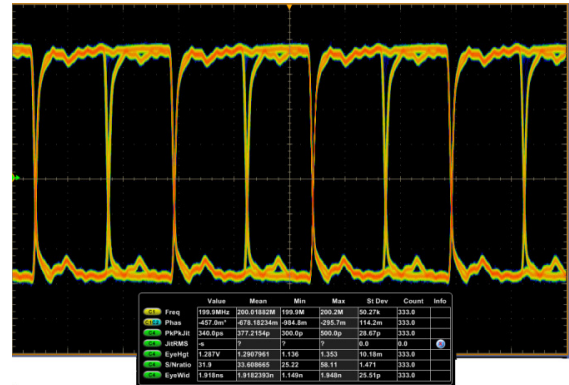


Fig.11. Eye diagrams for PWM signaling (200 Mbps, test channel 2): input signal and channel output signal.

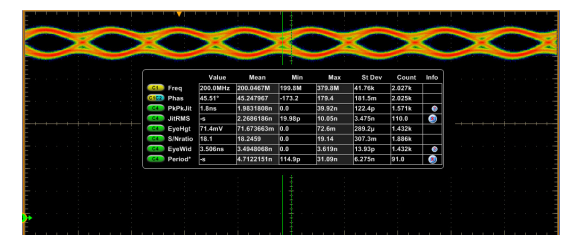
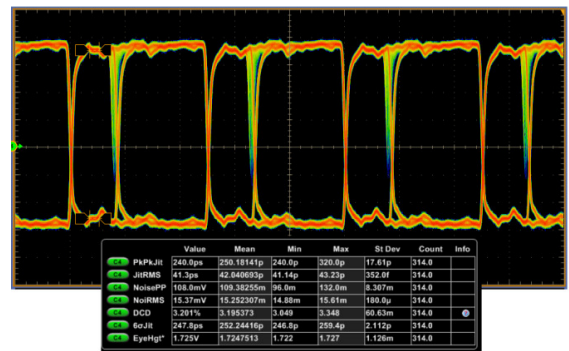


Fig.12. Eye diagrams for PWM-2 signaling (200 Mbps, test channel 2): input signal and channel output signal.

Note that the eye height, eye width, jitters and noise parameters are far better than in the case of PWM pulse, see Table 3. and Table 4. If both input pulses for PWM techniques are compared (only PCB trace from transmitter affects the data signal) it can be seen that the basic parameters like the eye height and jitter are very similar. However, it is obvious that PWM-2 signal has signal amplitude reduction from initial 1.800 V to 1.432 V (20.44 % reduction) and PWM signal has signal amplitude reduction from initial 1.800 V to 1.520 V (15.56 %

reduction). On the other hand comparison of both output eye diagrams brings better performance (more than 5 %) in eye height for PWM-2 signal, see Fig.13. and Fig.14. This confirms the correctness or reasoning that PWM-2 filter adjusts signal shaping similarly to the raised cosine approximation applied on PWM signal, and thus, signal goes through the channel with the same parameters with lower losses.

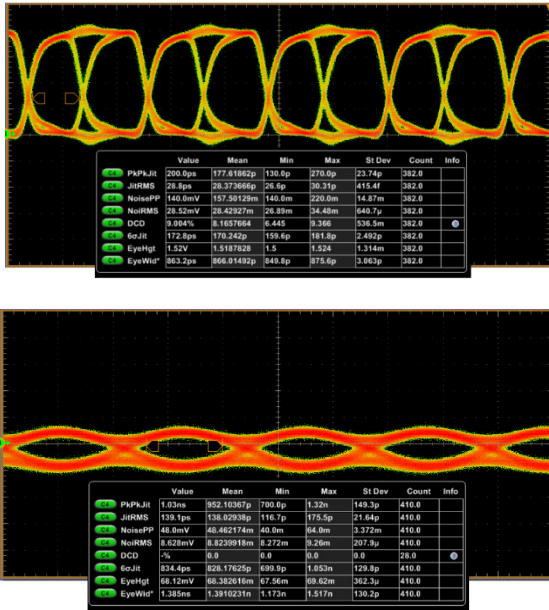


Fig. 13: Eye diagrams for PWM signaling (450 Mbps, test channel 1): input signal and channel output signal.

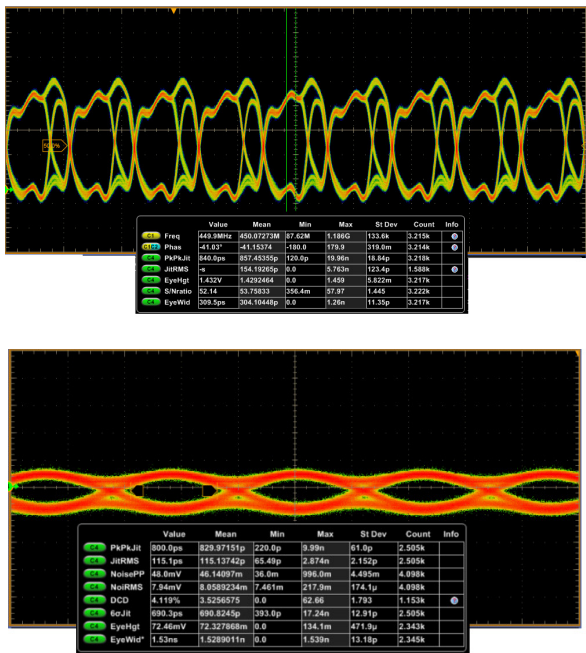


Fig.14. Eye diagrams for PWM-2 signaling (450 Mbps, test channel 1): input signal and channel output signal.

In Table 3. it is clearly demonstrated that during the lower transmission rates, where less channel low pass effect can be expected, the performance of PWM-2 techniques is not better in all parameters. Especially higher jitter and noise content due to more transitions in the PWM-2 signal is obvious. After the increasing of transmission rate, the low pass effect of transmission channel was increased significantly. Subsequently it can be seen that PWM-2 signaling is better adjusted for the higher channel losses, see results in Table 4.

Table 3. Performance of analyzed equalization techniques - 200 Mbps.

	$dc = 52\%$	$dc_1 = 28\%$ , $dc_2 = 90\%$	
200 Mbps	PWM	PWM-2	PWM-2 Performance
Eye width [ps]	3446	3506	+1.74%
Eye height [mV]	67.8	71.4	+5.3%
Jitter RMS [ps]	120.1	128.3	-6.6%
Noise RMS [mV]	16.5	18.2	-6.7%

Table 4. Performance of analyzed equalization techniques - 450 Mbps.

	$dc = 53\%$	$dc_1 = 29\%$ , $dc_2 = 76\%$	$dc = 50\%$	
450 Mbps	PWM	PWM-2	PWM	PWM-2 Perf.
Eye width [ps]	1385	1530	1182	+10.5 %
Eye height [mV]	68.12	72.46	42.76	+6.4%
Jitter RMS [ps]	139.1	115.1	173.3	+7.3%
NoiseRMS [mV]	8.63	7.94	13.84	+8%

6. CONCLUSION

In this paper both PWM and modified PWM-2 signaling methods were experimentally implemented and the final performance was compared. The presented results in section 4 clearly show the parameters of the analysed transmission channel and the presented eye diagrams show clearly the parameters of the analysed signal. In this case the conductive losses dominate in the transmission channel, see Fig.15. for illustration of experimental realization.

As can be seen from the performance comparison of PWM techniques listed in Table 3. and Table 4., the proposed PWM-2 scheme is able to achieve better eye opening at the Nyquist frequency of the transmitted pulse which corresponds to the current channel losses of about 35 dB. It is obvious that conventional PWM scheme does not achieve higher loss compensation than 30 dB and during the compensation of the 35 dB channel losses the eye diagram

shows worse results than in the case of PWM-2 filter. In Table 4. is clearly demonstrated that additional strong pre-emphasis ( $dc = 50\%$ ) is not able to improve the eye opening, and additional noise content which is generated results in eye closing. The PWM-2 scheme shows additional potential in future testing because the maximum  $dc$  coefficient settings are not achieved, especially  $dc_2$  coefficient set to only 76 has a reserve for compensation of pulses with longer tails. According to the carried-out simulation, the maximum limit of loss compensation should be more than 30 dB. Other works in the future will focus on implementation of modified PWM-2 scheme into the multi-level signaling variant which will be reliably comparable with a conventional PAM4 signaling scheme.

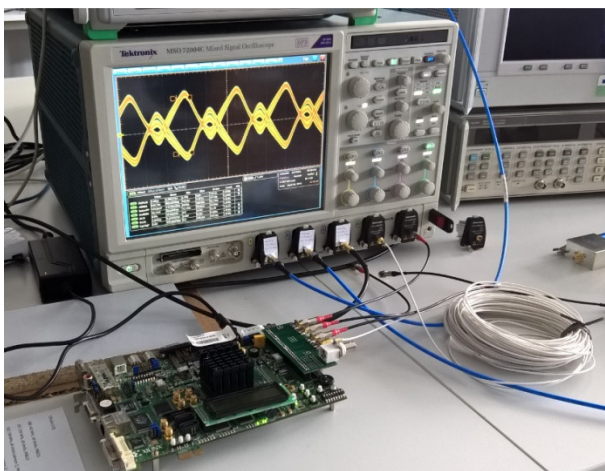


Fig.15. Experimental implementation - eye diagram for PWM signaling (450 Mbps) - weak pre-emphasis  $dc = 85\%$ .

#### ACKNOWLEDGMENT

This work was supported by Czech Science Foundation under grant 15-18288S. For research, infrastructure of the SIX Center was used.

#### REFERENCES

- [1] IEEE. (2014). *802.3bj-2014 - IEEE Standard for Ethernet Amendment 2: Physical Layer Specifications and Management Parameters for 100 Gb/s Operation Over Backplanes and Copper Cables*.
- [2] Chong, K.H.A., Avula, V., Liang, L., Pam, S., Mansour, M., Rao, F. (2014). IBIS AMI modeling of retimer and performance analysis of retimer based active serial links. In *DesignCon 2014*.
- [3] Zhang, H., Rao, F., Dong, X., Zhang, G. (2015). IBIS-AMI modeling and simulation of 56G PAM4 link systems. In *DesignCon 2015*.
- [4] Healey, A., Morgan, C.A. (2012). Comparison of 25 Gbps NRZ & PAM-4 modulation used in legacy & premium backplane channels. In *DesignCon 2012*.
- [5] Carrel, J., Barnes, H., Sleigh, R., Hakimi, H., Resso, M. (2014). De-mystifying the 28 Gb/s PCB channel: Design to measurement. *DesignCon 2014*.
- [6] Jin, L., Ling, X. (2004). Equalization in high-speed communication systems. *IEEE Circuits and Systems Magazine*, 4 (2), 4-17.
- [7] Ruifeng, S., Park, J., O'Mahony, F., Yue, C.P. (2005). A low-power, 20-Gb/s continuous-time adaptive passive equalizer. In *IEEE International Symposium on Circuits and Systems*, Cincinnati, Ohio, USA. IEEE, 920-923.
- [8] Gai, W., Hidaka, Y., Koyanagi, Y., Jiang, J.H., Osone, H., Horie, T. (2004). A 4-channel 3.125 Gb/s/ch CMOS transceiver with 30dB equalization. In *Symposium on VLSI Circuits, Digest of Technical Papers*, Honolulu, HI, USA. IEEE, 138-141.
- [9] Yuminaka, Y., Takahashi, Y., Henmi, K. (2009). Multiple-valued data transmission based on time-domain pre-emphasis techniques in consideration of higher-order channel effects. In *39th International Symposium on Multiple-Valued Logic*, Okinawa, Japan. IEEE, 250-255.
- [10] Schrader, J.H.R. (2010). *Wireline Equalization using Pulse-Width Modulation*. Ph.D. Thesis Series No. 07-104, Centre for Telematics and Information Technology (CTIT), Netherlands.
- [11] Yuminaka, Y., Henmi, K. (2010). Data-dependent time domain pre-emphasis techniques for high-speed data transmission. In *International Symposium on Communications and Information Technologies (ISCIT)*, Tokyo, Japan. IEEE, 1103-1107.
- [12] Ševčík, B., Brančík, L., Kubíček, M. (2011). Analysis of pre-emphasis techniques for channels with higher-order transfer function. *International Journal of Mathematical Models and Methods in Applied Sciences*, 5, 433-444.
- [13] Ševčík, B., Brančík, L. (2015). Signaling technique using inverse exponential function for high-speed on-chip interconnects. *WSEAS Transactions on Communications*, 14 (54), 470-476.
- [14] Ševčík, B., Brančík, L., Šotner, R., Kubíček, M. (2011). Signaling optimization techniques to reduce jitter and crosstalk susceptibility. *International Journal of Microelectronics and Computer Science*, 2 (3), 113-120.
- [15] Ševčík, B. (2012). Time-domain predistortion method based on raised cosine signaling in real transmission channels. *Active and Passive Electronic Components*, 2012 (1), 1-5.
- [16] Schrader, J., Klumperink, E., Nauta, B. (2006). Wireline equalization using pulse-width modulation. In *Custom Integrated Circuits Conference (CICC)*, San Jose, CA, USA. IEEE, 591-598.

Received January 16, 2017.

Accepted July 31, 2017.